minerals

MDPI

Article

Selenium Dissolution from Decopperized Anode Slimes in ClO^-/OH^- Media

Evelyn Melo *, María-Cecilia Hernández, Oscar Benavente and Víctor Quezada

Departamento de Ingeniería Metalúrgica y Minas, Universidad Católica del Norte, Antofagasta 1270709, Chile
* Correspondence: emelo@ucn.cl

Abstract: About 90% of selenium is obtained from treating copper anode slimes, which are a by-product of copper electrorefining. Selenium has been traditionally obtained by the pyrometallurgic treatment of anode slimes, which has been effective in recovery. However, in pyrometallurgical processes, there are increasingly strict environmental regulations. Hydrometallurgical treatments have been proposed to totally or partially replace conventional methods, some of which are in the developmental stage, while others are being used at the industrial scale. The selenium present in anode slimes is in the form of silver and copper selenides. This article proposes a hydrometallurgy alternative to recover selenium from decopperized anode slimes generated by a copper electrorefining plant in Chile by an alkaline-oxidizing leaching media (ClO^-/OH^-). The Taguchi experimental design was used to assess the effects of temperature, reagent concentration, and pH over time. The results indicated that the optimal selenium dissolution of 90% was achieved at pH 11.5, 45 °C, and 0.54 M of ClO^-. According to the SEM/EDX characterization of the solid leaching residue, the undissolved percentage of selenium is due to the generation of a layer of AgCl around the selenium particles that hinders the effective diffusion of the reagent.

Keywords: copper anode slimes; oxidative leaching; sodium hypochlorite; selenium; leaching

Citation: Melo, E.; Hernández, M.-C.; Benavente, O.; Quezada, V. Selenium Dissolution from Decopperized Anode Slimes in ClO^-/OH^- Media. *Minerals* **2022**, *12*, 1228. https://doi.org/10.3390/min12101228

Academic Editors: Kenneth N. Han and William Skinner

Received: 5 September 2022
Accepted: 23 September 2022
Published: 28 September 2022

1. Introduction

Selenium is found in most rocks and soils in the earth's crust. It is an essential material with a wide range of applications in medicine and the production of food, semiconductors, sensors, and photochemical devices. Selenium is rarely found in its native state, 90% being obtained from copper anode slimes, which are a byproduct of the copper electrorefining process [1–6].

During electrolysis, copper dissolved from the anode is deposited on the cathode. However, other elements in copper anodes, such as gold, silver, arsenic, antimony, selenium, tellurium, bismuth, lead, iron, and nickel are released from the anode. Some of these are soluble and accumulate in the solution, while the insoluble elements sink to the bottom of the cell and form raw anode slime [7], which is collected periodically from the bottom of the electrolytic cell for subsequent treatment [8,9].

Table 1 shows the ranges of the chemical elements in typical anodic slimes from refineries such as the Canadian Copper Refinery; Outokumpu (Finland); Saganoseki (Japan); Balkhash Mining-Metallurgical Combine (Kazakhstan); Kovoguty Krompakhi (Slovakia, closed); La Caridad Copper Refinery (Mexico); Jinchuan (China); Baiyin (China); and Ronnskar (Sweden) [10–14]. The elemental contents vary widely, depending on the origin of the anode slime.

Selenium is currently recovered from anode slimes by hydrometallurgical and pyrometallurgical processes [5,15,16]. Although the traditional pyrometallurgical method recovers selenium effectively, there are difficulties relating to high energy costs and increasingly strict environmental regulations [1,3,6,17,18]. Therefore, new alternatives have been

proposed, such as hydrometallurgical processes in oxidizing media such as nitric acid, alkaline leaching with sodium nitrate, wet chlorination, pressure leaching, sodium hydroxide, and acid leaching with MnO_2 or hydrogen peroxide, among others [1,2,4,6,9,17–20]. The hydrometallurgical process allows a better stabilization of selenium with respect to the pyrometallurgical process.

Table 1. Typical chemical composition of anodes slimes [10–14].

Element	Wt (%)
Cu	4.00–40.0
Se	0.70–21.0
Te	0.05–22.0
Pb	0.10–31.0
As	0.30–6.00
Fe	0.30–0.50
Bi	0.10–2.00
Ag	1.00–25.0
Au	0.004–2.00
Pt, Pd	<0.04

Selenium is commonly present in copper anodes as copper selenide (Cu_2Se), but in anode slimes, it occurs in various phases of Ag-Cu selenides [2,4,12,14–16,21]. Selenide is usually one of the main carriers of silver in anode slimes, this is because the silver in the solid copper matrix and the dissolved silver during electrorefining react with Cu_2Se to form Ag-Cu selenide compounds.

Ag-Cu selenides in anode slimes maintain the morphology of copper selenide (Cu_2Se) in the anode [12,14]. Small quantities of Te, S, and Au were detected in selenide particles and, according to the literature, almost all the Te, S, and Au initially present in the Cu_2Se of the copper anode remain in the selenides in anode slimes [9,14].

Sodium hypochlorite (ClO^-/OH^-) was used in several investigations as a highly oxidizing reagent that can be applied to leach chalcopyrite, enargite, and precious metals [22–27]. The authors [25,28] performed leaching experiments on enargite (Cu_3AsS_4) in ClO^-/OH^- media and found that arsenic dissolves and can be directly precipitated as a stable phase such as scorodite or as an amorphous ferric arsenate. According to [24], copper selenides (krutaite, $CuSe_2$) and gold telluride (calaverite, $AuTe_2$) are attacked by a ClO^-/OH^- system, dissolving selenium and tellurium, while copper and gold remain in the solid as tenorite (CuO) and elemental gold, respectively. Sodium hypochlorite was also widely used as an oxidant in various fields, for example, in flotation processes with ilmenite [29], the extraction of molybdenum from a Ni-Mo mineral by oxidant leaching [30,31], and the extraction of molybdenum from a copper concentrate [25].

The objective of this study is to evaluate the effect of the variables that influence the dissolution of selenium from decopperized anode slimes by alkaline oxidative leaching (ClO^-/OH^-). Considering the oxidative characteristics of sodium hypochlorite, in addition, this reagent has not been directly explored for the dissolution of selenium from anode slimes. Decopperized anode slime was obtained by the pretreatment of raw anode slime by agitated acid leaching with air injection. This paper does not analyze the decopperization process. The variables analyzed in this study are ClO^-/OH^- concentration, temperature, and pH.

2. Materials and Methods

2.1. Materials

The sample of decopperized anode slime used in this work was obtained from a large Chilean electrolytic refinery. The sample was washed three times with distilled water to remove impregnated soluble copper and acid, and the solid sample was dried at 343 K (70 °C) for subsequent chemical analysis by atomic absorption spectrometry (AAS) (Perkin Elmer, model PinAAcle 500, Singapore) and X-ray diffraction (XRD) (Siemens model D5600,

Bruker, Billerica, MA, USA) with an analysis time of one hour. The ICDD (International Centre for Diffraction Data, Version PDF-2, Bruker, Billerica, MA, USA) database was used to identify the phases present, and the TOPAS (total pattern analysis software, Version 2.1, Bruker, Billerica, MA, USA) program was used for quantification. The XRD equipment uses an internal corundum standard. Scanning electron microscopy (SEM) (JEOL USA Inc., Peabody, MA, USA) with dispersive X-ray energy spectroscopy (EDX) (Zeiss Ultra Plus, Zeiss, Jena, Germany) was used to determine particle size.

The copper anode slimes were characterized in an earlier work [8], which indicated that the average particle size was 11 μm, and contained the following main elements: Se (10.9%), Cu (0.97%), As (0.92%), Pb (1.1%), Sb (1.1%), Au (0.23%), and Ag (0.49%). The main phases in the decopperized anode slime were selenium, such as CuAgSe, and phases of Ag-Se, $Ag_{(2-x)}Se$, Sb-As-O, and antimony arsenate, $AsSbO_4$, as well as phases of $BaSO_4$ and AgCl.

2.2. Leaching Experiments

The leaching experiments were conducted in a 500 mL, four-necked glass reactor at atmospheric pressure, with 10 g of the sample treated in a 250 mL solution. The central reactor opening had a mechanical stirrer with a digital display screen (IKA, model RW20, Staufen im Breisgau, Germany). Temperature, pH, and Eh were measured using a pH-ORP meter (Hanna Instrument, HI 3221, Padova, Italy), which was inserted in a lateral neck of the reactor. The system was placed in a thermostatic bath (Julabo, model MP-19A, St. Louis, MO, USA) to maintain the required temperature. A 25 mL microburette was used to add sodium hydroxide (NaOH, 3 M) and sulfuric acid (H_2SO_4, 1 M) through the lateral neck to control the pH level. The aqueous solution was sampled at 5, 15, 30, 60, and 120 min of leaching to measure selenium and hypochlorite concentrations. Selenium was measured by AAS and Flow Injection System (FIAS) for hydride generation and hypochlorite by iodometric titration. The parameters of the study varied from 0.27, 0.4, and 0.54 M of ClO^-; 25, 35, and 45 °C; and pH 11.5, 12.0, and 12.5. All experiments were run at a stirring speed of 300 min^{-1}. At the end of the leaching, the product solution and residue were filtered. The leaching residue was washed three times with distilled water and then dried in a drying oven at 70 °C for 24 h. Experiments were performed in duplicate, and the results presented here are the averages of the obtained data (±2.0% in selenium dissolution). In addition, the elements of the experimental setup can be identified in Figure 1 (e.g. reactor, stirrer, pH-ORP meter, thermostatic bath, etc.).

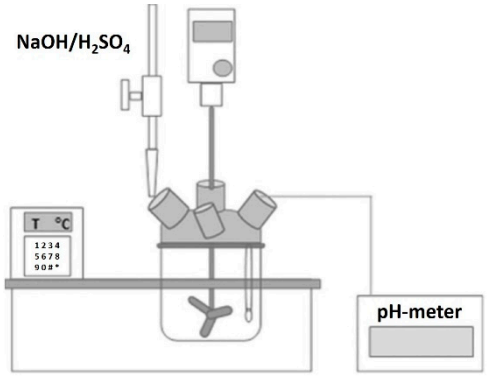

Figure 1. Experimental setup.

The residue leaching sample was briquetted with epoxy resin, polished, and coated with carbon. The briquette obtained was analyzed using scanning electron microscopy (SEM) (JEOL, model JSM 840) with dispersive X-ray energy spectroscopy (EDX), which provides information on elemental analysis and the morphology of the different phases.

2.3. Taguchi Experimental Design

The Taguchi optimization method was used to determine the optimal combination of variables. Three factors and three levels were evaluated in the experiments, as shown in Table 2:

Table 2. Leaching conditions with sodium hypochlorite.

Level/Factor	Low (1)	Medium (2)	High (3)
Temperature in °C	25.0	35.0	45.0
[ClO^-], M	0.27	0.40	0.54
pH	11.5	12.0	12.5
Agitation, min^{-1}	300	300	300

The application of the orthogonal Taguchi matrix yielded the L_{27} experimental model to evaluate the reaction progress (see Table 3) and the L_9 model to identify the optimal combination of variables. This orthogonal array was selected because of its potential to pattern the interactions among the factors. Table 4 shows the experimental design developed in this research (L_9).

Table 3. Experimental model to evaluate the reaction progress, L_{27} (effects).

Test No.	Temperature, °C	ClO^-, M	pH
1	25.0	0.54	11.5
2	35.0	0.27	11.5
3	35.0	0.27	12.5
4	25.0	0.54	12.5
5	25.0	0.27	11.5
6	45.0	0.54	11.5
7	45.0	0.54	12.5
8	45.0	0.40	12.5
9	45.0	0.40	12.0
10	45.0	0.27	11.5
11	25.0	0.40	11.5
12	35.0	0.40	11.5
13	35.0	0.54	11.5
14	25.0	0.54	12.0
15	35.0	0.54	12.0
16	25.0	0.40	12.5
17	35.0	0.54	12.5
18	25.0	0.27	12.5
19	45.0	0.40	11.5
20	25.0	0.40	12.0
21	35.0	0.40	12.5
22	45.0	0.54	12.0
23	35.0	0.40	12.0
24	25.0	0.27	12.0
25	45.0	0.27	12.5
26	35.0	0.27	12.0
27	45.0	0.27	12.0

Table 4. Taguchi experimental design (L_9) to determine the optimal combination of leaching with sodium hypochlorite.

Test No.	Temperature, °C	ClO^-, M	pH
1	25.0	0.27	11.5
2	35.0	0.27	12.0
3	45.0	0.27	12.5
4	35.0	0.40	11.5
5	45.0	0.40	12.0
6	25.0	0.40	12.5
7	45.0	0.54	11.5
8	25.0	0.54	12.0
9	35.0	0.54	12.0

3. Results and Discussion

3.1. Effect of Temperature

The effect of temperature on the Se leaching was evaluated at 25, 35, and 45 °C. Figure 2 shows the results in terms of the selenium dissolution with an initial sodium hypochlorite concentration of 0.54 M. The selenium dissolution increased slightly in the first 15 min due to an increase in temperature and then continued to increase for up to 120 min as temperature increased, reaching a dissolution of 90% at 45 °C. During the advance of the reaction, an effect of the temperature with respect to the concentration of ClO^- was observed. This is because of the high reagent concentration, which leaves the ClO^- available at 45 °C, generating a slow decomposition of the reagent [31]. According to [25], the temperature has a significant effect on the dissolution of arsenic from enargite with ClO^-/OH^-, reaching an extraction of 65% in 30 min. According to [28], the temperature has a significant effect on leaching molybdenum in sodium hypochlorite, with extractions of 83% and 99.9% at 20 and 50 °C, respectively. However, the accelerated decomposition of ClO^-/OH^- begins to occur at temperatures above 50 °C [32]. These results show that sodium hypochlorite is highly oxidizing and an effective reagent for dissolving selenium.

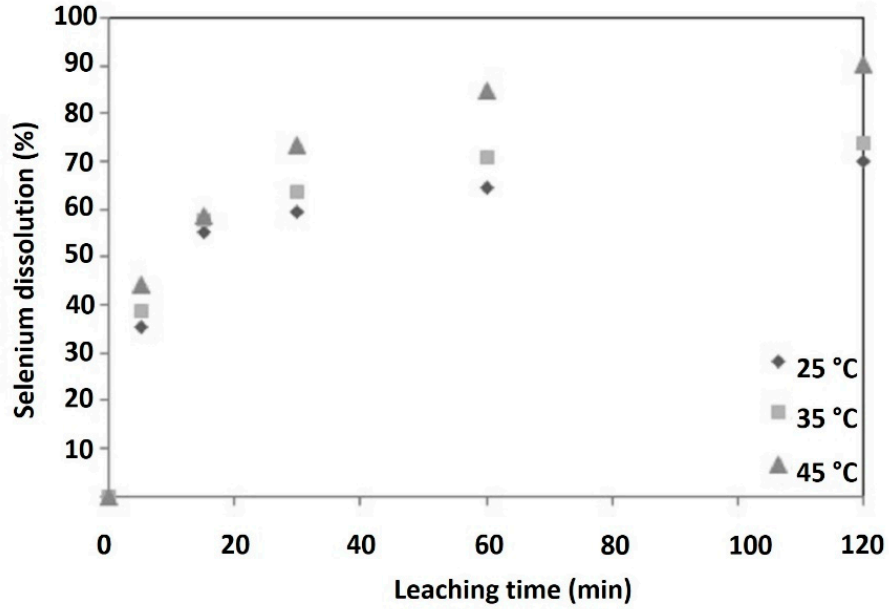

Figure 2. Effect of temperature on leaching selenium [ClO^-] = 0.54 M; pH 11.5.

3.2. Effect of the Sodium Hypochlorite Concentration

The sodium hypochlorite concentrations were 0.27 M; 0.4 M and 0.54 M. The reaction was measured with the variable of selenium dissolution. Figure 3 shows that the results obtained with 0.27 and 0.4 M of ClO^- at 120 min were not significantly different, representing selenium dissolution of 66 and 69%, respectively. The concentration of 0.54 M shows a significant increase in dissolution compared to the lower concentrations, resulting in a selenium dissolution of 90%. According to [25], they observed similar behavior, with an increase in the concentration of ClO^- having a favorable effect on the reaction of enargite in an alkaline media, which demonstrated that the reaction of enargite is electrochemical. In the study published by [31], the molybdenum extraction increased significantly (from 16.3% to 99.99%) with an increase in ClO^- concentration.

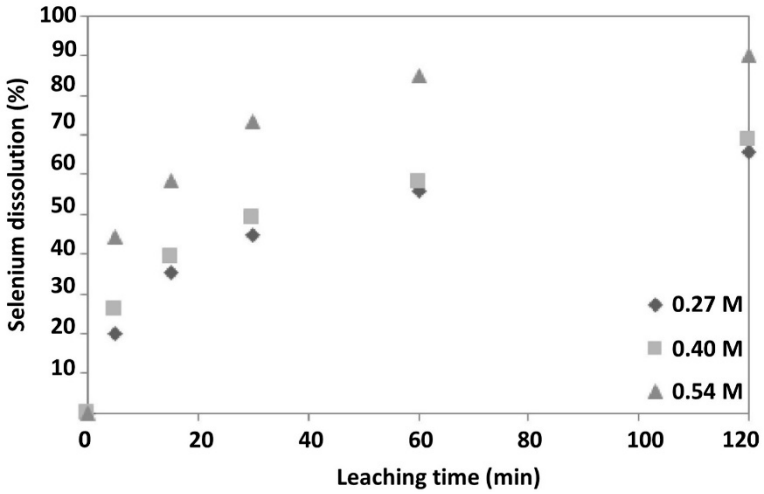

Figure 3. Effect of sodium hypochlorite concentration at pH 11.5 and 45 °C.

3.3. Effect of pH

Leaching experiments were conducted with three pH levels, 11.5, 12.0, and 12.5, with 0.54 M of ClO^- at 45 °C, to determine the effect of pH on the selenium dissolution over time. Figure 4 shows the results of the experiments. Figure 4 shows the evident favorable effect of a decrease in the pH level. A selenium dissolution of 90% was obtained at pH 11.5, which was significantly higher than the dissolution (63%) at pH 12.5. According to [25], hypochlorite decomposition increases significantly at pH levels above 12.5, which can explain the low selenium dissolution rate under this parameter.

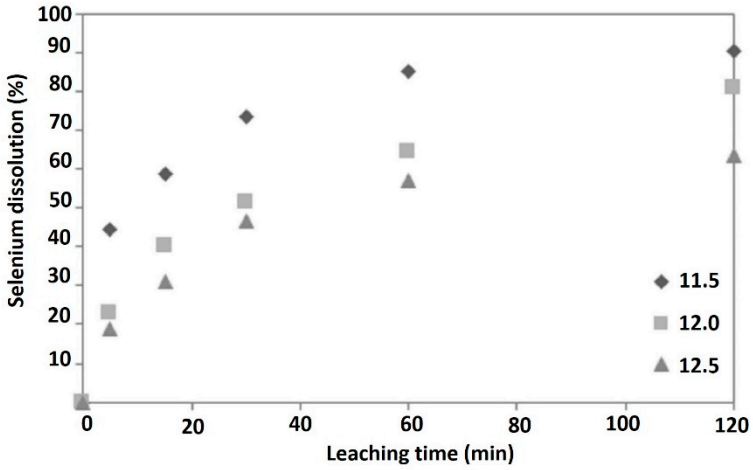

Figure 4. Effect of the pH level on leaching selenium, with 0.54 M of ClO^- at 45 °C.

3.4. Optimizing Leaching in a Sodium Hypochlorite Media

The selenium dissolutions obtained were evaluated with a Minitab 18 computational tool (Minitab LLC, State College, PA, USA) in accordance with the Taguchi experimental model. Table 5 presents the average selenium dissolutions for each level of the evaluated variable.

Table 6 and Figure 5 show the statistical data for the average selenium dissolution for each effect evaluated (ClO^-, pH, and T °C). The first data point in Figure 5 represents the average of the selenium dissolution for all the tests in which the concentration of ClO^- is classified as level 1 (0.27 M) (see Table 5, tests 1, 2, and 3). The second data point of the ClO^- effect represents the average of selenium dissolution for the tests at level 2 (see Table 5, tests 4, 5, and 6). The third data point represents the average at level 3 (see Table 5, tests 7, 8, and 9).

Table 5. Response to the Taguchi experimental model.

Test No.	ClO^-, M	pH	Temperature, °C	Se dissolution, %
1	0.27	11.5	25.0	53.36
2	0.27	12.0	35.0	51.57
3	0.27	12.5	45.0	29.81
4	0.40	11.5	35.0	60.10
5	0.40	12.0	45.0	65.57
6	0.40	12.5	25.0	35.08
7	0.54	11.5	45.0	90.17
8	0.54	12.0	25.0	65.60
9	0.54	12.5	35.0	59.82

Table 6. Average response to the evaluated variables.

	Selenium Dissolution, %		
Level	**ClO^-**	**pH**	**Temperature**
Low (1)	44.91	67.88	51.35
Medium (2)	53.58	60.91	57.16
High (3)	71.86	41.57	61.85

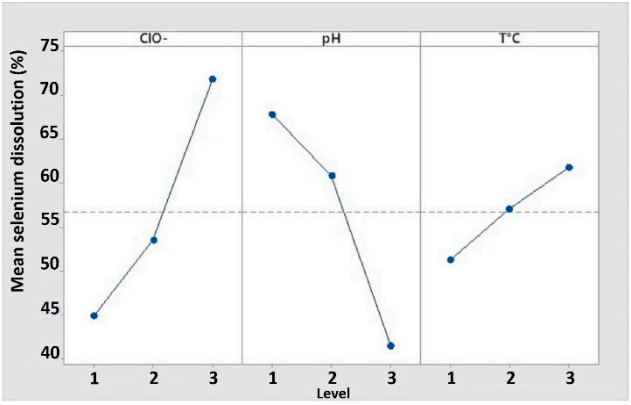

Figure 5. Effect of the parameters: ClO^-, pH, and temperature.

The effect of pH in Figure 5 is also represented by three data points: the first data point shows the average selenium dissolution at level 1 (pH 11.5; tests 1, 4, and 7 from Table 5); the second data point at level 2 (pH 12; tests 2, 5, and 8 from Table 5); and the third data point at level 3 (pH 12.5; tests 3, 6, and 9 from Table 5). The same procedure was applied for temperature.

The average selenium dissolution (%), the maximum for each effect, is the best condition—that is, for this experiment, the best combination is 0.54 M of ClO^-, pH 11.5, and a temperature of 45 °C, which were the parameters in experiment No. 7 (Table 5). The selenium dissolution under these conditions was 90.17%.

Figure 5 shows that the variables ClO^- and pH have the greatest effect on the selenium dissolution, with pH 12.5 giving the lowest dissolution.

The results of leaching decopperized anode slime in a ClO^-/OH^- media indicated that selenium is largely dissolved in the alkaline solution. Although the oxidation state of selenium cannot be determined, it is possible to find Se(IV) and Se(VI) based on redox potentials above 0.5 V (SHE) [33]. In this study, in the tests performed, the Eh values were in the range of 0.8–0.9 V vs SHE.

3.5. SEM/EDX Characterization of Leaching Residues

The leaching residues were vacuum filtered and washed three times with distilled water after each experiment to eliminate any soluble elements that remained from the

leaching. The residue from the leaching with optimal results was selected for analysis (pH 11.5, at 45 °C and 0.54 M of ClO^-). The entire briquette was scanned at two points with a magnification of ×250 (Figure 6c,d) and ×350 (Figure 6a,b) using SEM with backscattered electron reading (BES), which revealed homogeneity in the present phases. The granulometry was not uniform as the result of the formation of agglomerates of fine particles (<35 µm) after chemical crushing compared to decopperized anode slimes [8].

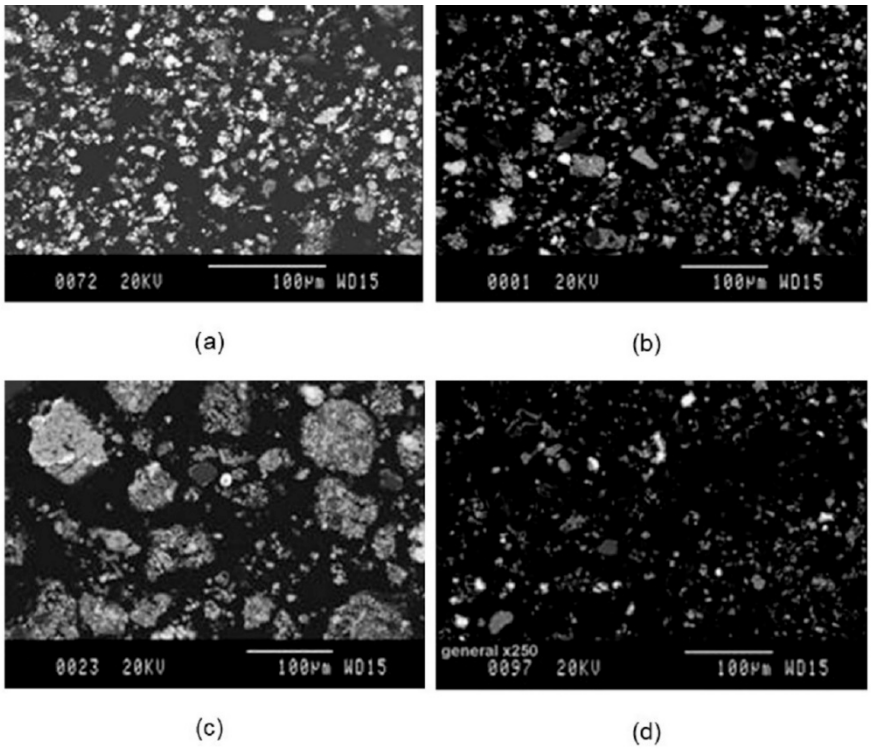

Figure 6. SEM image of leaching residue. ×350: (**a**,**b**). ×250: (**c**,**d**).

Figure 7 shows the spectrum from the analysis of the image of the leaching residue in ClO^-/OH^- media at a magnification of ×350 (from the sample of Figure 6b), and Table 7 shows a semi-quantitative analysis.

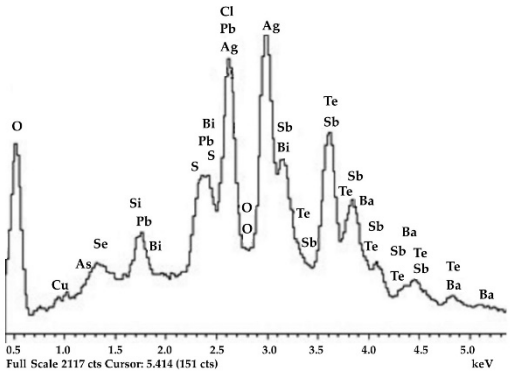

Figure 7. General EDX spectrum of residues from leaching ClO^-/OH^-.

Figure 7 shows the most significant elements in the ClO^-/OH^- leaching residue, which are Ag, Pb, Sb, and Cl. As, Cu, Se, Bi, Te, and Ba are present in smaller quantities. Barium is present because it is used as a release agent in copper anode molding. Au was not detected because it is a trace element that cannot be detected at the magnification at which the analysis was conducted (×350), according to Figure 6b.

Table 7. Semi-quantitative analysis of residues from leaching ClO^-/OH^-.

Element	Weight, %	Atomic, %
O	16.42	52.40
Si	1.75	3.19
S	0.94	1.50
Cl	8.12	11.69
Cu	1.63	1.31
As	1.76	1.20
Se	1.21	0.79
Ag	24.35	11.52
Sb	24.68	10.35
Te	5.45	2.18
Ba	4.11	1.53
Pb	5.72	1.41
Bi	3.84	0.94

Figure 6 shows the elements in different shades of black and white. The phases with elements with higher atomic numbers are closer to white, therefore lead, barium, and silver are in light tones. With the higher magnification of these particles (×600), the image reveals that the majority of phases are composed of Ag, Pb, Sb, and Se (Figure 8).

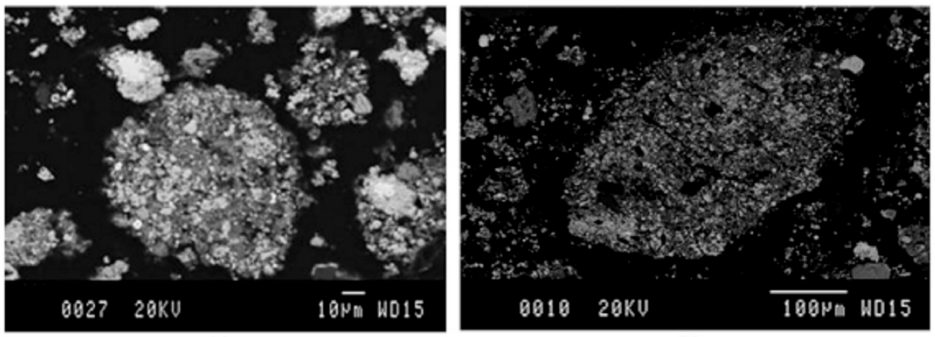

Figure 8. Representative areas of anode slime ClO^-/OH^- (×600). (**a**) the particle size is between 10 µm and 50 µm, (**b**) The particle size is between 10 µm and 400 µm.

The different phases in the leaching residue can be observed in Figure 8, which shows attacked particles (Figure 8a,b) agglomerated oxidized phases with varying contents of Se, Pb, Ag, and Cl. The particle size is between 10 µm and 400 µm, as shown in Figure 8b. This is because it has been leached, and therefore the particle size is smaller than that of particles in the slime that were initially fed into the leaching [8], which resulted in the formation of agglomerates.

3.5.1. Phase Ba-S-O

Barium is homogeneously distributed throughout the sample, with a variable size of 2 µm (Figure 9a), reaching sizes of 50 µm, as shown in Figure 9b. The barium phase (barium sulfate) was present in the anode slime before leaching in ClO^-/OH^- media [8], which remained without reaction after leaching in oxidizing alkaline media. The elements were quantified in an analysis using particles of approximately 50 µm (Figure 9b), which allowed for reliable results. Table 8 shows the results of the analysis, which were the average values of three analyses of the central particle shown in Figure 9b. According to the quantification in atomic percentages, the ratio between Ba and S is 1:1, which confirms the presence of barium sulfate. The spectrum in Figure 10 shows these elements.

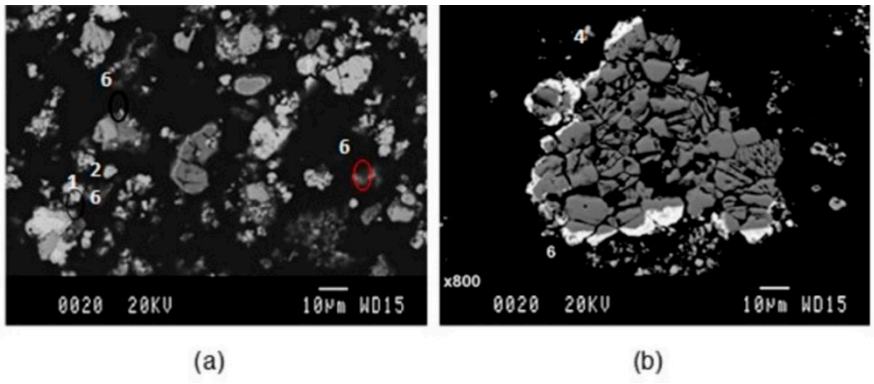

Figure 9. Pb-rich particles of $BaSO_4$ (phase 6), AgCl (phase 2), Ag-Cl-Se, and Sb-Pb-O (phase 4). Variable size between 2 µm (**a**) and 50 µm (**b**).

Table 8. Semi-quantitative analysis of Ba-S-O.

Element	Weight, %	Atomic, %
O	21.23	58.64
S	15.15	20.88
Ba	63.62	20.48

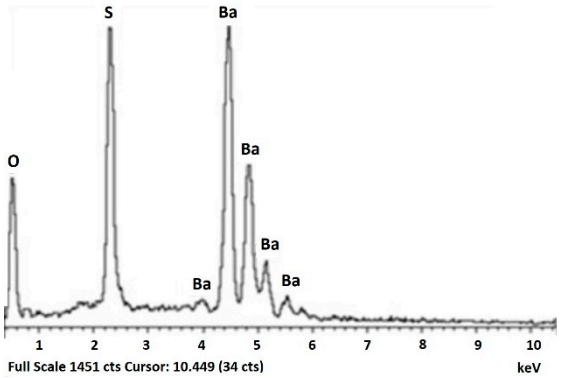

Figure 10. Spectrum and quantification associated with Ba-S-O particles.

The Figure 9, Figure 11 and Figure 13 identify the phases with the following numbering: 1 (Ag_2Se), 2 (AgCl), 3 (O-Pb-Ag), 4 (a, b, c) (O-Sb-Pb-Ag, Cl), 6 ($BaSO_4$).

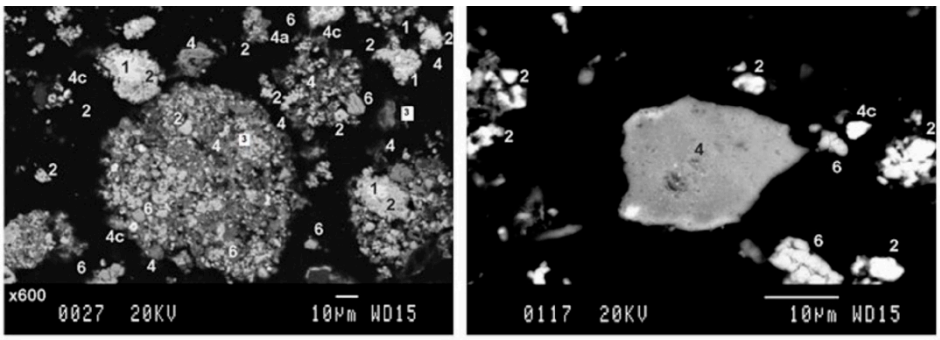

Figure 11. Oxidized O-Sb-Pb (phase 4) (with traces of Cu-Bi-Cl-Ag).

3.5.2. Oxidized Phases

The area in Figure 6d was scanned and oxidized areas were detected. These areas are in isolated form or as an amorphous mass that serves as the basis for the formation of other

phases, as shown in Figure 11. Figure 12 shows the spectrum of the oxidized phases, in which there are O-Sb-Pb phases associated with traces of Cu-Bi-Cl-Ag.

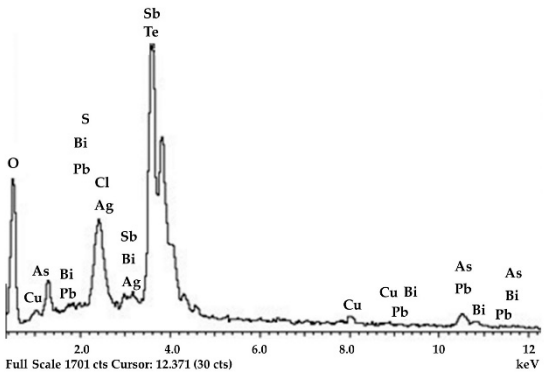

Figure 12. Spectrum of the oxidized O-Sb-Pb phase (with traces of Cu-Bi-Cl-Ag).

In much of the leached slimes, there were oxidized phases that differed from each other in terms of the composition and quantity of elements present. According to the analysis by the researchers of this work, decopperized anode slime has the following behavior during oxidative alkaline leaching:

The decopperized slime fed into the leaching in ClO^-/OH^- media had a remnant AgCuSe content [8] that formed oxidized phases of the same during the leaching.

The following Equations (1) and (2) can be hypothesized.

$$AgCuSe + 4.5ClO^- + OH^- \rightarrow AgCl + CuO + SeO_4^{2-} + 3.5Cl^- + 0.5H_2O \quad (1)$$

$$AgCuSe + 3.5ClO^- + OH^- \rightarrow AgCl + CuO + SeO_3^{2-} + 2.5Cl^- + 0.5H_2O \quad (2)$$

In previous studies, the research team found that the lead in the decopperized slime is in the form of anglesite $PbSO_4$ [8], which reacts in the ClO^-/OH^- media according to Equation (3).

$$PbSO_4 + 2OH^- \rightarrow PbO + SO_4^{2-} + H_2O \quad (3)$$

There can be a remnant phase of As-Sb-O, rich in Sb and poor in As, compared to decopperized slime, in which As-Sb-O formed $AsSbO_4$ [8]. The reason for this is that As is soluble in an oxidizing alkaline media [22,25].

3.5.3. Silver Selenide and Silver Chloride Phases

The selenium phases in the residues are presented as an Ag-Se phase associated with Ag-Cl and isolated traces of the Ag-Se phase. Traces of selenium remain trapped in the Ag-Cl phase because the reaction progresses through the AgCl layers, which does not allow the reagent to diffuse. Consequently, the reactions that govern the selenium phases can be hypothesized by Equations (4) and (5). These reactions are thermodynamically possible given that they have a Gibbs free energy of -174.228 kcal (Equation (4)) and −134.143 kcal (Equation (5)). Equation (4) is more spontaneous than Equation (5).

$$Ag_2Se + 4ClO^- \rightarrow 2AgCl + SeO_4^{2-} + 2Cl^- \quad (4)$$

$$Ag_2Se + 3ClO^- \rightarrow 2AgCl + SeO_3^{2-} + Cl^- \quad (5)$$

Several selenide particles can be seen surrounded by AgCl (Figure 13). Figure 14 and Table 9 show examples of quantification and EDX analysis, respectively. This allowed for determining that the selenide phase of the decopperized slime, $Ag_{(2-x)}Se$ [8], was not attacked because of the AgCl layer that surrounds it.

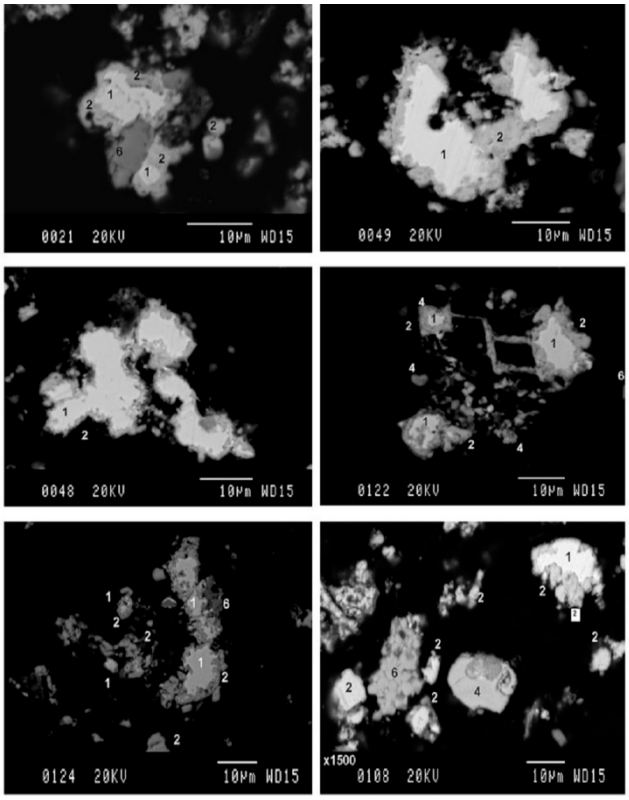

Figure 13. Silver selenide Ag_2Se (phase 1), AgCl (phase 2), O-Sb-Pb (phase 4), $BaSO_4$ (phase 6).

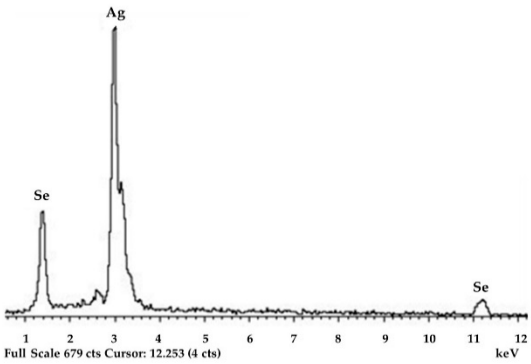

Figure 14. Spectrum associated with the Se-Ag phase (phase 1).

Table 9. Semi-quantitative analysis of the Se-Ag phase (phase 1).

Element	Weight, %	Atomic, %
Se	29.92	36.84
Ag	70.08	63.16

The EDX analysis (Figure 15) at the edge of the particles (phase 2) shown in Figure 13 determined that the selenide is surrounded by AgCl. The semi-quantitative analysis shown in Table 10 indicates an atomic Ag:Cl ratio of 1:1. The AgCl layer did not allow the effective diffusion of the reagent in the pH 11.5 leaching tests, 45 °C and 0.54 M, resulting in the slow kinetics of the system at 60 min. Given the above, it is proposed to evaluate a two-stage leaching process or to increase the reaction time.

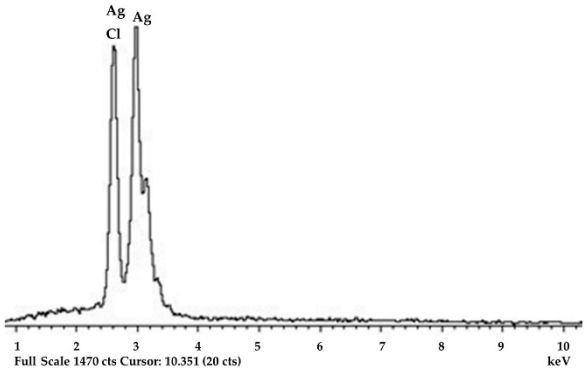

Figure 15. Spectrum associated with Ag-Cl (phase 2).

Table 10. Semi-quantitative analysis of the Ag-Cl phase.

Element	Weight, %	Atomic, %
Cl	24.55	49.75
Ag	75.45	50.25

4. Conclusions

The Levels of pH of 11.5 and 12 have a positive effect on selenium dissolution, yielding 90 and 80% dissolution, respectively. The dissolution decreases at pH 12.5, reaching a maximum of 60% since the hypochlorite decomposition increases significantly at pH levels above 12.5. A ClO^-/OH^- concentration of 0.54 M significantly affects the selenium dissolution, reaching values of over 60%, with a maximum of 90%, for all the evaluated parameters of pH and temperature. However, no significant effect on selenium dissolution was observed over time for concentrations 0.27 and 0.4 M, and at pH 11.5 and a temperature of 45 °C. The temperature was noted to affect selenium dissolution in the assessed range of 25 °C to 45 °C. The best results of 74 and 90% dissolution were obtained at 35 and 45 °C, respectively. The temperature has a significant effect on the dissolution of selenium. However, temperatures above 50 °C accelerated the decomposition of ClO^-/OH^-. The best conditions for dissolving selenium are pH 11.5; 45 °C and 0.54 M of ClO^-, which yields a dissolution of 90%, according to the Taguchi design The selenium was not completely dissolved because a layer of AgCl is generated around the selenium particles ($Ag_{(2-x)}Se$) during leaching that obstructs the progress of the reaction. Ag, Pb, Sb, and Cl compounds were detected as major phases in the leaching residue from the test at pH 11.5, 45 °C, and 0.54 M of ClO^-. Silver was found mainly as AgCl. Lead sulfate became lead oxide. The arsenic phase present in the decopperized anode as $SbAsO_4$ decreases after leaching with ClO^-/OH^-. This occurs because arsenic dissolves in alkaline oxidizing media.

Our results at the laboratory level indicate that hypochlorite is an interesting reactant for dissolving selenium from anode slime, and the pyrometallurgic stage can be replaced by hydrometallurgical process under moderate conditions.

Author Contributions: Conceptualization, E.M. and M.-C.H.; methodology, E.M.; software, O.B.; validation, E.M. and M.-C.H.; formal analysis, V.Q.; investigation, E.M.; resources, E.M.; data curation, E.M.; writing—original draft preparation, E.M.; writing—review and editing, V.Q.; visualization, V.Q.; supervision, E.M.; project administration, O.B.; funding acquisition, M.-C.H. All authors have read and agreed to the published version of the manuscript.

Funding: This research was funded by Fondecyt, N° 1030872, Conicyt, Chile.

Data Availability Statement: Not applicable.

Acknowledgments: The authors are grateful for the funding from the Fondecyt project 1030872 "Tecnología sostenible para el tratamiento de barros anódicos" and to the Grup de Recerca en Caracterització i Processat en Ciència dels Materials of the Universitat de Barcelona (CPCM). We are also grateful to Joan Viñals (RIP) of the Universitat de Barcelona for all his support in characterizing the leaching residues.

Conflicts of Interest: The authors declare no conflict of interest.

References

1. Dong, Z.; Jiang, T.; Xu, B.; Yang, J.; Chen, Y.; Li, Q.; Yang, Y. Comprehensive recoveries of selenium, copper, gold, silver and lead from a copper anode slime with a clean and economical hydrometallurgical process. *Chem. Eng. J.* **2020**, *393*, 124762. [CrossRef]
2. Xiao, L.; Wang, Y.; Yu, Y.; Fu, G.; Liu, Y.; Sun, Z.; Ye, S. Enhanced selective recovery of selenium from anode slime using MnO_2 in dilute H_2SO_4 solution as oxidant. *J. Clean. Prod.* **2019**, *209*, 494–504. [CrossRef]
3. Xiao, L.; Wang, Y.; Yu, Y.; Fu, G.; Han, P.; Sun, Z.; Ye, S. An environmentally friendly process to selectively recover silver from copper anode slime. *J. Clean. Prod.* **2018**, *187*, 708–716. [CrossRef]
4. Yang, H.-Y.; Li, X.-J.; Tong, L.-L.; Jin, Z.-N.; Yin, L.; Chen, G.-B. Leaching kinetics of selenium from copper anode slimes by nitric acid-sulfuric acid mixture. *Trans. Nonferrous Met. Soc. China* **2018**, *28*, 186–192. [CrossRef]
5. Lu, D.-K.; Chang, Y.-F.; Yang, H.-Y.; Xie, F. Sequential removal of selenium and tellurium from copper anode slime with high nickel content. *Trans. Nonferrous Met. Soc. China* **2015**, *25*, 1307–1314. [CrossRef]
6. Kilic, Y.; Kartal, G.; Timur, S. An investigation of copper and selenium recovery from copper anode slimes. *Int. J. Miner. Process.* **2013**, *124*, 75–82. [CrossRef]
7. Wang, X.; Chen, Q.; Yin, Z.; Wang, M.; Xiao, B.; Zhang, F. Homogeneous precipitation of As, Sb and Bi impurities in copper electrolyte during electrorefining. *Hydrometallurgy* **2011**, *105*, 355–358. [CrossRef]
8. Melo, E.; Hernández, M.C.; Viñals, J.; Graber, T. Characterization of Raw and Decopperized Anode Slimes from a Chilean Refinery. *Metall. Mater. Trans. B* **2016**, *47*, 1315–1324. [CrossRef]
9. Hait, J.; Jana, R.K.; Sanyal, S.K. Processing of copper electrorefining anode slime: A review. *Miner. Process. Extr. Met.* **2009**, *118*, 240–252. [CrossRef]
10. Chen, A.; Peng, Z.; Hwang, J.-Y.; Ma, Y.; Liu, X.; Chen, X. Recovery of Silver and Gold from Copper Anode Slimes. *JOM* **2015**, *67*, 493–502. [CrossRef]
11. Chen, T.T.; Dutrizac, J.E. Mineralogical characterization of a copper anode and the anode slimes from the la caridad copper refinery of mexicana de cobre. *Met. Mater. Trans. B* **2005**, *36*, 229–240. [CrossRef]
12. Chen, T.T.; Dutrizac, J.E. Mineralogical characterization of anode slimes-9. The reaction of Kidd Creek Anode Slimes with various lixiviants. *Can. Metall. Q.* **1993**, *32*, 267–279. [CrossRef]
13. Chen, T.T.; Dutrizac, J.E. The mineralogy of copper electrorefining. *JOM* **1990**, *42*, 39–44. [CrossRef]
14. Chen, T.T.; Dutrizac, J.E. MIneralogical characterization of anode slimes-II. Raw anode slimes from inco's copper cliff copper refinery. *Can. Metall. Q.* **1988**, *27*, 97–105. [CrossRef]
15. Kanari, N.; Allain, E.; Shallari, S.; Diot, F.; Diliberto, S.; Patisson, F.; Yvon, J. Thermochemical Route for Extraction and Recycling of Critical, Strategic and High Value Elements from By-Products and End-of-Life Materials, Part I: Treatment of a Copper By-Product in Air Atmosphere. *Materials* **2019**, *12*, 1625. [CrossRef]
16. Kanari, N.; Allain, E.; Shallari, S.; Diot, F.; DiLiberto, S.; Patisson, F.; Yvon, J. Thermochemical Route for Extraction and Recycling of Critical, Strategic and High-Value Elements from By-Products and End-of-Life Materials, Part II: Processing in Presence of Halogenated Atmosphere. *Materials* **2020**, *13*, 4203. [CrossRef]
17. Li, X.J.; Hong, Y.Y.; Zhe, N.J.; Guo, B.C.; Lin, L.T. Transformation of Selenium-Containing Phases in Copper Anode Slimes During Leaching. *JOM* **2017**, *69*, 1932–1938. [CrossRef]
18. Li, X.-J.; Yang, H.-Y.; Jin, Z.-N.; Tong, L.-L.; Xiao, F.-X.; Chen, G.-B. Extraction of selenium from copper anode slimes in a sealed leaching system. *Metall. Rare Noble Met.* **2017**, *58*, 357–364. [CrossRef]
19. Kim, D.; Wang, S. *Developments in Copper Anode Slimes-Wet Chlorination-Processing*; Copper: Hamburg, Germany, 2010.
20. Kurniawan, K.; Lee, J.-C.; Kim, J.; Kim, R.; Kim, S. Leaching Kinetics of Selenium, Tellurium and Silver from Copper Anode Slime by Sulfuric Acid Leaching in the Presence of Manganese (IV) Oxide and Graphite. *Mater. Proc.* **2021**, *3*, 16. [CrossRef]
21. Chen, T.T.; Dutrizac, J.E. Mineralogical characterization of anode slimes: Part 7-copper anodes and anode slimes from the Chuquicamata Division of Codelco-Chile. *Can. Metall. Q.* **1991**, *30*, 95–106. [CrossRef]
22. Garlapalli, R.K.; Cho, E.H.; Yang, R.Y. Leaching of Chalcopyrite with Sodium Hypochlorite. *Met. Mater. Trans. A* **2009**, *41*, 308–317. [CrossRef]
23. Baghalha, M. Leaching of an oxide gold ore with chloride/hypochlorite solutions. *Int. J. Miner. Process.* **2007**, *82*, 178–186. [CrossRef]
24. Benavente, O.; Hernández, M.C.; Viñals, J.; Roca, A.; Herreros, O. *Removal of Arsenic, Tellurium and Selenium from Copper and Precious Metal Concentrates*; Alta Copper: Perth, Australia, 2005.
25. Viñals, J.; Roca, A.; Hernández, M.; Benavente, O. Topochemical transformation of enargite into copper oxide by hypochlorite leaching. *Hydrometallurgy* **2003**, *68*, 183–193. [CrossRef]

26. Jeffrey, M.I.; Breuer, P.L.; Choo, W.L. A kinetic study that compares the leaching of gold in the cyanide, thiosulfate, and chloride systems. *Met. Mater. Trans. B* **2001**, *32*, 979–986. [CrossRef]
27. Puvvada, G.; Murthy, D. Selective precious metals leaching from a chalcopyrite concentrate using chloride/hypochlorite media. *Hydrometallurgy* **2000**, *58*, 185–191. [CrossRef]
28. Herreros, O.; Quiroz, R.; Hernández, M.C.; Viñals, J. Dissolution kinetics of enargite in dilute Cl_2/Cl^- media. *Hydrometallurgy* **2002**, *64*, 153–160. [CrossRef]
29. Cai, J.; Deng, J.; Wen, S.; Zhang, Y.; Wu, D.; Luo, H.; Cheng, G. Surface modification and flotation improvement of ilmenite by using sodium hypochlorite as oxidant and activator. *J. Mater. Res. Technol.* **2020**, *9*, 3368–3377. [CrossRef]
30. Liu, W.; Xu, H.; Yang, X.; Shi, X. Extraction of molybdenum from low-grade Ni–Mo ore in sodium hypochlorite solution under mechanical activation. *Miner. Eng.* **2011**, *24*, 1580–1585. [CrossRef]
31. Liu, Y.; Zhong, H.; Cao, Z. Molybdenum removal from copper ore concentrate by sodium hypochlorite leaching. *Min. Sci. Technol.* **2011**, *21*, 61–64.
32. Adam, L.C.; Gordon, G. Hypoclorite ion decomposition: Effects of temperature, ion strength, and chloride ion. *Inorg. Chem.* **1999**, *38*, 1299–1304. [CrossRef]
33. Burriel, F.; Lucena, F.; Arribas, S.; Hernández, J. *Química Analítica Cualitativa*, 18th ed.; Thomson Editores: Spain, Madrid, 2008; pp. 567–570.